

RESEARCH

Open Access



# *Xoo*-responsive transcriptome reveals the role of the circular RNA133 in disease resistance by regulating expression of *OsARAB* in rice

Kuaifei Xia<sup>1,2†</sup>, Xiaoqing Pan<sup>1,3,4†</sup>, Xuan Zeng<sup>1,2\*</sup> and Mingyong Zhang<sup>1,2\*</sup> 

## Abstract

Upon *Xanthomonas oryzae* pv. *oryzae* (*Xoo*) infection of rice leaves, the invasion induces systematic expression changes for both the coding genes and the non-coding genes, allowing the plant to make corresponding responses. However, the roles of circular RNAs (circRNAs) in rice defending against *Xoo* remain largely unknown. To address this question, we conducted a whole-transcriptomic analysis to systematically screen the differentially expressed (DE) mRNAs and non-coding RNAs (ncRNAs) in rice responding to *Xoo* infection. Our results revealed a total of 4076 DE mRNAs, 89 DE long non-coding RNAs (lncRNAs), 82 DE microRNAs (miRNAs), and 14 DE circRNAs identified from *Xoo*-infected rice plants at 48 h post inoculation. Three circRNAs (ciR52, ciR298, and ciR133) were found to be able to form circular RNAs, and their expression was induced by *Xoo* infection. ciR133 was found to repress the expression of its parental gene *OsARAB* (putative arabinofuranosidase gene) during *Xoo* infection. Overexpression of ciR133 and mutation of *OsARAB* enhanced rice resistance against *Xoo*, without compromising main agronomic traits. Our data suggest that circRNAs are associated with rice response to *Xoo* infection, providing a potential strategy for breeding *Xoo*-resistant rice plants by manipulating ciR133 and *OsARAB*.

**Keywords** Rice, Bacterial blight, *Xanthomonas oryzae* pv. *oryzae*, circRNA, ncRNA

## Background

*Oryza sativa* L. (Rice) is one of the most important crops, feeding more than half of the world's population. *Xanthomonas oryzae* pv. *oryzae* (*Xoo*) is a devastating bacterial disease on rice, causing yield loss up to 50% in Asia and Africa (Adhikari et al. 1995; Ahmed et al. 2020). *Xoo* first enters rice leaves through wounds or margins, and then moves to the leaf xylem, leading to the plant wilting and yield loss (Wang et al. 2017; Oliva et al. 2019). Transferring resistance (R) genes into different rice cultivars has been demonstrated to be the most effective and economical strategy to control *Xoo* infection (Sun et al. 2004; Buddhachat et al. 2022). To date, more than 40 R genes have been identified in rice, and 14 of which have

<sup>†</sup>Kuaifei Xia and Xiaoqing Pan contributed equally to this work.

\*Correspondence:

Xuan Zeng

zengxuan@scbg.ac.cn

Mingyong Zhang

zhangmy@scbg.ac.cn

<sup>1</sup> Key Laboratory of South China Agricultural Plant Molecular Analysis and Genetic Improvement & Guangdong Provincial Key Laboratory of Applied Botany, South China Botanical Garden, Chinese Academy of Sciences, Guangzhou 510650, China

<sup>2</sup> South China National Botanical Garden, Guangzhou 510650, China

<sup>3</sup> University of Chinese Academy of Sciences, Beijing 10049, China

<sup>4</sup> Present Address: Hans Knöll Institute A1, Adolf Reichwein Street 23, 07745 Jena, Germany



been cloned, including *Xa1* (Yoshimura et al. 1998), *Xa21* (Pruitt et al. 2015), and *Xa23* (Wang et al. 2015).

Endogenous non-coding RNAs (ncRNAs) have been implicated in the interaction of rice resistance to *Xoo* infection (Lu et al. 2021; Song et al. 2021). Overexpression of miR169o in rice reduced the disease resistance to *Xoo* by decreasing the transcription of defense genes (Yu et al. 2018). miR1861k may play a role in broad spectrum resistance to *Xoo* (Zhang et al. 2015). Down-regulation of miR156 and overexpression of its two targets *IPAI* and *OsSPL7* enhanced rice resistance to *Xoo* infection (Liu et al. 2019). The *Xoo*-induced long ncRNA (lncRNA) *ALEX1* up-regulates the expression of jasmonate (JA)-responsive genes, such as *JAZ8* and *MYC2*, and mediates the increased endogenous levels of JA to enhance resistance against *Xoo* (Yu et al. 2020).

The covalently closed circular RNAs (circRNAs) were first reported in virus in 1975 (Takahashi and Diener 1975), and later they have been identified in almost all eukaryotes and prokaryotes (Li et al. 2018). Advances in next-generation sequencing have enabled the identification of circRNAs in *Arabidopsis*, rice, soybean, wheat, maize, and many other plant species (Lai et al. 2018). circRNAs are formed by canonical back-splicing of gene introns or exons from precursor mRNA, and their biogenesis is catalyzed and modulated by RNA binding proteins and flanking intronic complementary sequences (Li et al. 2018). Because of their special topological structure, circRNAs are more stable than other RNAs (Chen et al. 2019a). Generally, circRNAs are expressed at lower levels than linear RNAs or other ncRNAs, but they show more variants due to alternative splicing (Feng et al. 2019). Although the functions of most circRNAs remain largely unexplored, they are known to sequester miRNAs or proteins, and modulate gene transcription. The first reported functional circRNA in eukaryotes is ciRS-7, which was identified to act as a miRNA sponge to inhibit miR-7 function in human brains (Hansen et al. 2011; Memczak et al. 2013). Circ-*MALAT1* in mammalian cancer stem cells was observed to function as a *PAX5* mRNA translation brake by competing with the ribosomes entry site (Chen et al. 2019a). In *Arabidopsis*, a circRNA derived from exon 6 of the *SEPALLATA3* (*SEP3*) gene was demonstrated to pause transcription of its cognate DNA locus by forming an RNA:DNA or R-loop (Conn et al. 2017). In rice, *CircR5g05160* was found to be induced by *Magnaporthe oryzae* infection, which consequently promoted the immunity in rice (Fan et al. 2020). However, the response of circRNAs to *Xoo* infection in rice is not known yet.

Plants must protect their cell walls from penetration by bacterial and fungal pathogens that seek access to the nutrient-rich environment within the cell. The plant

cell wall is dynamic, and its structure and composition are changed during pathogen infection, partially due to modification by microbial cell wall-degrading enzymes (Zhao and Dixon 2014). Plants have developed a dedicated mechanism to maintain cell wall integrity which could be utilized to enhance crop disease resistance (Bacete et al. 2018). Primary cell walls are composed of three polysaccharides: cellulose, hemicelluloses, and pectin, which determine the cell shape and mechanical strength. Lignin, a phenylpropanoid polymer, is deposited in the cell wall during secondary wall thickening (Brown et al. 2005). Arabinofuranosidases (ARABs) are enzymes that catalyze the hydrolysis of terminal, non-reducing  $\alpha$ -L-arabinofuranoside residues, and contribute to reduce the number of links between lignin and cell wall polysaccharides, and to degrade lignin-carbohydrate complexes (Hashimoto et al. 2011). Transgenic rice plants expressing *ARAB* (*ARAF*) from *Coprinopsis cinerea* displayed the reduced ferulate-lignin cross-links by detaching arabinose side chains from arabinoxylan and the increased abundance of alkaline-resistant benzyl ether cross-links (Maruyama et al. 2021). Overexpression of rice *OsARAF1* and *OsARAF3* led to an increase in cellulose accumulation and saccharification efficiency, including an increase in arabinose content and a decrease in glucose content; however, it does not affect modifications of cell wall polysaccharides (Sumiyoshi et al. 2013). Polygalacturonase depolymerizes pectin by hydrolysis, thereby altering pectin composition and structure and activating cell wall defense. Loss-of-function mutation of *ltn-212* destroyed cell wall integrity, resulting in spontaneous cell death and an auto-activated defense responses, including reactive oxygen species burst and pathogenesis-related gene expression, as well as enhanced resistance to *Xoo* infection (Cao et al. 2021). Knocking out of transcription factor *WRKY53* thickens sclerenchyma cell walls of the vascular bundle, conferring the resistance to *Xoo* (Xie et al. 2021).

In the present study, our transcriptomic analysis revealed that a total of 4076 mRNAs, 82 miRNAs, 89 lncRNAs, and 14 circRNAs displayed differential expression in rice seedlings after 48 h of *Xoo* infection. An analysis for transgenic rice showed that ciR133 could repress expression of its parental gene *OsARAB*, and plays a positive role in defending against *Xoo* infection. Therefore, *ciR133* and *OsARAB* may be the candidate genes that can be used for *Xoo*-resistance breeding in rice plants.

## Results

### Transcriptomic analysis of rice plants infected by *Xoo*

One-month-old rice leaves were treated with *Xoo* strain AXO1947 and H<sub>2</sub>O, and were harvested two days later for transcriptomic sequencing (Fig. 1a). Pair-end

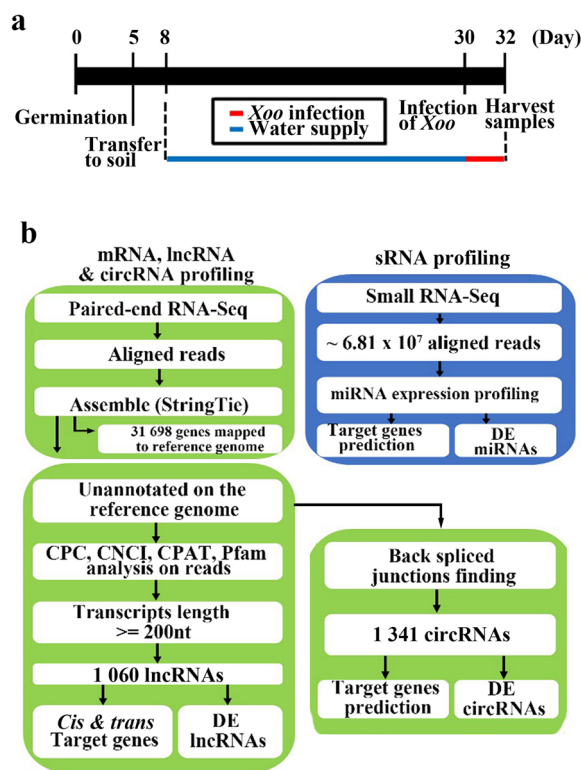


**Fig. 1** Flow chart of whole transcriptomic RNA-sequencing. **a** The workflow of wild type rice ZH11 infected by *Xanthomonas oryzae* (*Xoo* African strain AXO1947). Thirty-day-old plants were treated with *Xoo* and H<sub>2</sub>O for 48 h for RNA extraction. The experiment was repeated with three biological replicates. **b** The schematic diagram for the generation of two cDNA libraries, RNA sequencing, and analysis of differentially expressed (DE) genes

RNA-Sequencing was used to identify mRNAs, lncRNAs, and circRNAs, while small RNA-Sequencing was used to identify miRNAs (Fig. 1b). Quality control of the 6 RNA samples yielded 108.80 Gb of clean data, with Q30 percentages higher than 93.47% and GC contents ranging from 43.86% to 45.25%. Subsequently, 740 million clean reads were generated and mapped to the rice genome (IRGSP-1.0), resulting in unique alignment rates ranging from 27.79% to 37.11% for total RNA-seq (Additional file 1: Table S1). To validate the RNA-seq data, real-time quantitative PCR (RT-qPCR) was used to examine the expression of five up-regulated and five down-regulated genes on differentially expressed (DE) mRNAs, and non-coding RNAs (lncRNAs and miRNAs) (Additional file 2: Figure S1). The results showed that the DE mRNAs, lncRNAs, and miRNAs identified from the RNA-sequencing could be verified by RT-qPCR.

A total of 31,698 mRNAs, 1,060 lncRNAs, 691 miRNAs, and 1,341 circRNAs candidates were expressed in the rice seedlings treated with *Xoo* (Additional file 1: Table S2). All of them are listed in Additional file 1: Tables

S3–S6. Of them, 1358 new genes are sequenced (Additional file 1: Table S3), and 253 new miRNAs are found (novel miRs in Additional file 1: Table S5). After filtering the protein-coding RNAs (mRNAs) based on prediction by multiple software, we predicted that the majority of lncRNAs (624 lncRNAs) were intergene-lncRNAs, while the rest were antisense-lncRNAs, intronic-lncRNAs, and sense-lncRNAs.

### The transcriptome of *Xoo*-infected rice plants

Analysis of DE mRNAs and ncRNAs after *Xoo* infection revealed a total of 4076 mRNAs, 89 lncRNAs, 82 miRNAs, and 14 circRNAs with altered expression, including 2041, 52, 39, and 10 up-regulated mRNAs, lncRNAs, miRNAs, and circRNAs respectively, and 2035, 37, 43, and 4 down-regulated mRNAs, respectively (Additional file 1: Table S2). All of the DE RNAs are listed in Additional file 1: Tables S7–S10.

Combined analysis of DE lncRNAs with DE miRNAs and mRNAs revealed that 78 DE lncRNAs co-expressed with the target DE *Cis*-mRNAs, 4 DE miRNAs co-expressed with their target DE lncRNAs, and three DE lncRNAs (MSTRG.26116.1, MSTRG.38793.1, and MSTRG.9627.3) co-expressed with the target DE *Cis*-mRNAs and DE miRNAs simultaneously (Additional file 1: Table S11 and Additional file 2: Figure S2a). All 89 DE lncRNAs co-expressed with target DE *trans*-mRNAs, and 4 DE lncRNAs (MSTRG.11997.2, MSTRG.26116.1, MSTRG.38793.1, and MSTRG.9627.3) co-expressed with target DE *trans*-mRNAs and DE miRNAs simultaneously (Additional file 2: Figure S2b and Additional file 1: Table S11). Based on the targeted genes of DE lncRNAs and DE miRNAs, the KEGG annotation suggests five categories, including cellular process, environmental information processing, genetic information processing, metabolism, and organismal systems (Additional file 2: Figures S2c, S3).

The DE mRNAs include some known pathogenesis-related genes, such as *PR10a* and *OsSWEET14* (Additional file 1: Table S12), while the DE miRNAs include rice immunity related miRNAs, such as miR169a and miR528 (Additional file 1: Table S13) which have been reported in pathogen-infected rice (Li et al. 2014). These data indicate that *Xoo* infection can cause significant changes in gene expression. The combined analysis of DE miRNAs and DE mRNAs, among the 82 DE miRNAs and 4,076 DE mRNAs after *Xoo* infection, indicated that there are 33 down-regulated miRNAs and their putative target genes are up-regulated; however, there are 7 up-regulated miRNAs and their putative target genes are down-regulated (Table 1). This result suggests that these miRNAs play important roles in response to *Xoo* infection by regulating the putative target genes.

**Table 1** All differentially expressed (DE) miRNAs in rice ZH11 plants by combined analysis with the eligible predicted target DE mRNAs after 48 h of *Xoo* infection

Down-regulated miRNAs	Up-regulated putative targeted genes and their annotation
novel_miR_92	Os07g0603100 (Nuclear transport factor 2); Os01g0365000 (Wall-associated receptor kinase 5); Os05g0446600 (DNA glycosylase 704); Os11g0173500 (Probable LRR receptor-like serine/threonine-protein kinase); <i>Oryza_sativa_newGene_4972</i> (Disease resistance protein RPM1); Os05g0446000 (Exonuclease VII small subunit); Os11g0590700 (Disease resistance protein RPP13); Os11g0565000 (LRR receptor-like serine/threonine-protein kinase FLS2); Os09g0482640 (Wall-associated receptor kinase 3); Os11g0127600 (Probable helicase MAGATAMA 3); Os12g0178700 (Dynamin-like protein ARC5); Os10g0155500 (Aldose 1-epimerase); Os12g0203900; Os01g0763100 (RNA processing and modification)
miR528-5p	Os09g0365900 (L-ascorbate oxidase); Os04g0688500 (Cationic peroxidase SPC4); Os11g0167300 (NYN domain; OST-HTH/LOTUS domain)
miR162b	Os03g0127600 (Transcription factor activity, sequence-specific DNA binding); Os07g0182900 [DNA (cytosine-5)-methyltransferase]
miR395a	Os09g0567900 (Probable inactive methyltransferase); Os04g0104900 (Translation, ribosomal structure and biogenesis); Os01g0266000 (Posttranslational modification, protein turnover, chaperones)
miR395p, 395q, 395r, 395 m, 395 l, 395n, 395 k, 395b, 395i, 395 h, 395j, 395y, 395d, 395e, 395 g, 395 s	Os09g0567900 (Nucleotide transport and metabolism)
miR395f	Os03g0151700 (Similar to WD repeat protein); Os01g0266000 (RNA-binding protein)
miR156j-3p	Os08g0558900 (Enzyme inhibitor activity)
miR408-5p	Os11g0189600 (Lipid transport and metabolism); Os10g0538200 (Aspartic proteinase nepenthesin-1); Os10g0537800 (Aspartic proteinase nepenthesin-1)
novel_miR_108	<i>Oryza_sativa_newGene_10065</i> (Uncharacterized protein LOC4346670 isoform X3)
miR1428g-5p, 1428e-5p, 1428f-5p	Os01g0885000 (Cytochrome C oxidase, cbb3-type, subunit III)
miR5079a, 5079b	Os10g0577600 (JmjC domain, hydroxylase)
miR1428e-3p	<i>Oryza_sativa_new gene_7640</i> (Putative receptor protein kinase ZmPK1)
miR528-3p	Os02g0132100 (Pentatricopeptide repeat-containing protein); Os05g0133100 (Nitrogen regulatory protein P-II);
miR2118r, 2118e	<i>Oryza_sativa_new gene_717</i>
Up-regulated miRNAs after <i>Xoo</i> infection	Putative down-regulated targeted genes
miR2871a-3p, 2871b-3p	Os02g0663300 (BEACH domain containing protein)
miR169r-5p	Os01g0759900 (Nucleobase-ascorbate transporter 2)
miR1861c	Os10g0160000 (Ubiquitin carboxyl-terminal hydrolase 10); Os01g0856900 (Disease resistance RPP13-like protein 4)
miR169a	Os01g0236300 (Auxin response factor 1)
miR5542	Os02g0143200 (Armadillo-type fold domain containing protein); Os03g0249200 (RF-1 domain)
miR172c	Os12g0177800 (S-Domain receptor like protein-12)

### Expression change of circRNAs after *Xoo* infection

A total of 1341 circRNA candidates were identified from rice seedlings using the find\_circ and CIRI2 software packages (Fig. 2a and Additional file 1: Tables S2, S6). The majority (85%) of the parental genes of circRNAs produced only one circRNA, while some generated two to eight (Fig. 2b). The length of circRNAs ranged from 200 to over 3000 nucleotides (nt). Exonic circRNAs were mostly abundant in 400 nt, while a few intergenic circRNAs were longer than 3000 nt (Fig. 2c). The average expression level of circRNAs before *Xoo* infection was higher than that after 48 h of *Xoo* infection (Fig. 2d).

The find\_circ and CIRI software were used to analyze the DE circRNAs in response to *Xoo*-infection. A total of 14 DE circRNAs were found from rice seedlings after 48 h of *Xoo* infection (Fig. 2a, b and Table 2). Only one up-regulated and one down-regulated circRNA were identified by two software, which are chr03:11550445|11551137 (ciR133), and chr06:16279995|1680386 (Fig. 3a). Of the 14 DE circRNAs, and seven genes were generated from parental genes, namely Os03g0320100 (a-L-arabinofuranosidase), Os04g0684500 (*OsWSL5*), Os04g0686650, Os06g0480200, Os07g0672500, Os09g0268300 (Hexose carrier), and Os09g0343200. circRNAs and other noncoding RNAs cannot function independently in

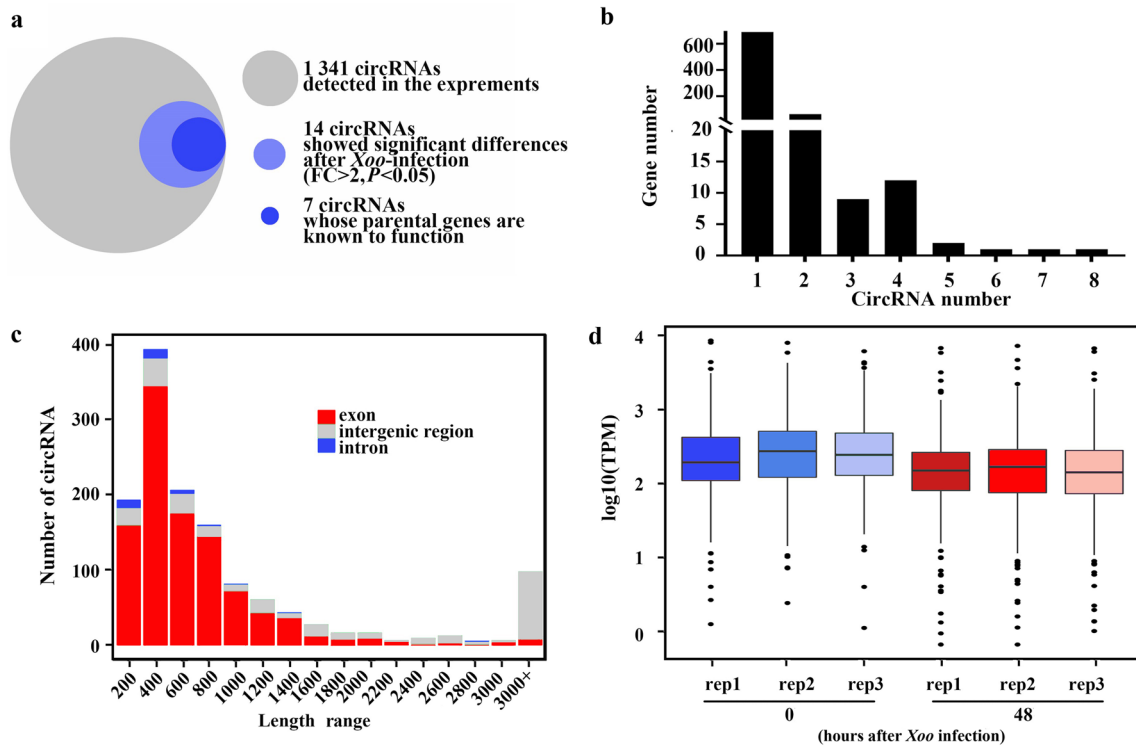


**Fig. 2** Summary of circRNAs in ZH11 seedlings after *Xoo* infection. **a** Identification of differentially expressed (DE) circRNAs after *Xoo* infection. A total of 1,341 circRNAs were detected, and 14 of which showed differential expression ( $FC > 2$  and  $P < 0.05$ ) after *Xoo* infection. Seven of the DE circRNAs were predicted to derive from the known functional parental genes. **b** Number of genes capable of producing 1–8 circRNAs. **c** Number of circRNAs with different lengths and circRNAs are produced from different locations of genes. **d** Average expression level (transcripts per million, TPM) of all circRNAs in ZH11 and *Xoo*-infected ZH11

**Table 2** Differentially expressed circRNAs in rice ZH11 plants after 48 h of *Xoo* infection

ID of circRNAs	Expression level (FPKM)		Change	Parental genes
	Before	<i>Xoo</i> infection		
3:11550445 11551137 (ciR133)	0	4722 ± 2395	Up	Os03g0320100 (a-L-arabinofuranosidase)
4:31276588 31301714	0	237 ± 79	Up	
3:267628 268062 (ciR52)	27,428 ± 3023	54,844 ± 7270	Up	
11:6657912 6707725	65 ± 34	146 ± 64	Up	
4:35093089 35095669 (ciR298)	3270 ± 1484	8797 ± 2854	Up	Os04g0686650
9:10618503 10619042	2712 ± 3134	10,231 ± 3401	Up	Os09g0268300 (Hexose carrier)
9:5140146 5140580	0	2099 ± 1110	Up	Os09g0343200
4:24014063 24014278	0	4723 ± 2048	Up	
1:18152219 18153178	0	1692 ± 880	Up	
7:28426090 28427266	0	1851 ± 1372	Up	Os07g0672500
6:2448727 2448878	20,522 ± 18,735	0	Down	
6:1627995 16280386	4840 ± 2127	0	Down	Os06g0480200
8:27930611 27963872	592 ± 8	0	Down	
4:34965141 34969807	4949 ± 1711	1428 ± 471	Down	Os04g0684500 ( <i>OsWLS5</i> , white stripe leaf 5)

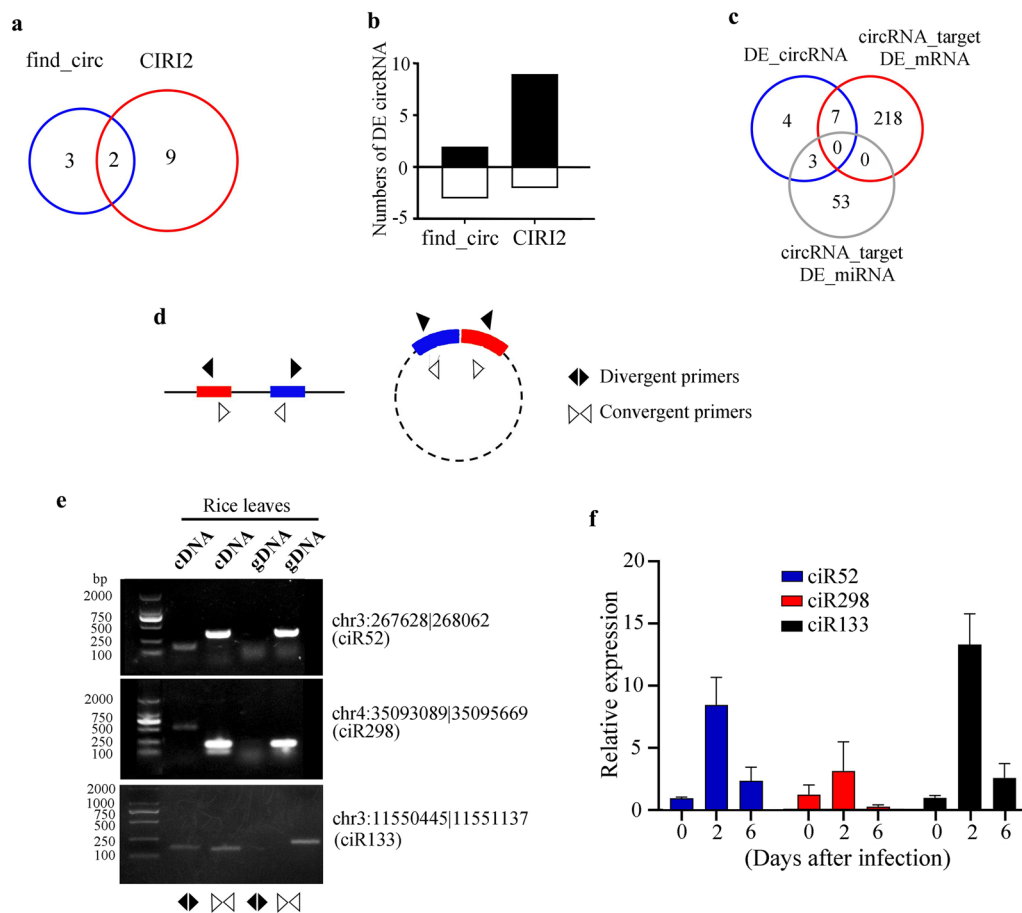


**Fig. 3** Validation of the differentially expressed (DE) circRNAs in rice plants after *Xoo*-infection. **a** Number of DE circRNAs after *Xoo*-infection were identified by find\_circ and CIRI2 software. **b** Number of the up- and down-expressed circRNAs after *Xoo*-infection. **c** Number of the potential network prediction of circRNA-miRNA-mRNA. The DE circRNAs were used for predicting the target mRNAs and miRNAs. **d-f** Validation of circular RNA formation of 3 circRNAs by (RT)-PCR assays. **d** PCR diagram using genomic DNA (left) and circular cDNA (right) of circRNAs as template. **e** The electrophoretogram of circular RNA formation of 3 circRNAs by (RT)-PCR assays. The circular cDNA of circRNAs (ciR52, ciR298, and ciR133) could be amplified by divergent primers (first column), but not their genomic DNA (gDNA) (third column). Circular cDNA from circRNAs and gDNA of the parental genes could be amplified by the convergent primers (second and fourth columns). **f** Expression change of the DE circRNAs in ZH11 after *Xoo* infection using divergent primers in RT-qPCR assays. *OseEF1-a* was used as a reference gene. Means  $\pm$  SD represent the value with standard deviation (n = 3 biological repeats)

plants, so we further studied and analyzed the relationship between circRNAs, DE miRNAs, and DE mRNAs through bioinformatics (Fig. 3c). We found that 225 circRNAs potentially target DE mRNAs, and 55 circRNAs have putative miRNA binding sites. Further analysis predicted that three DE circRNAs may interact with DE miRNAs (chr4:2014063|24014278, chr4:31276588|31301714, chr8:27930611|27963872) to form a DE circRNA-DE miRNA network, and seven DE circRNAs may interact directly with DE mRNAs (3:11550445|11551137, 4:35093089|35095669, 9:10618503|10619042, 9:5140146|5140580, 7:28426090|28427266, 6:16279995|16280386, 4:34965141|34969807) to form a DE circRNA-DE mRNA network.

Because the divergent primer pair for RT-PCR can amplify bands from the circular RNAs but not from linear RNAs and the convergent primer pair can detect the linear RNAs but not circular RNAs (Fig. 3d), these primer pairs were used to distinguish circRNAs from linear RNAs or linear DNAs by PCR and RT-qPCR (Fig. 3e, f). Three circular RNAs (ciR52, ciR298, and ciR133) could be amplified using the divergent primer pair when cDNAs were used as templates, but not gDNAs as templates. However, their parental genes can be amplified with the convergent primer pair when cDNAs and gDNAs were used as templates (Fig. 3e). The result showed that ciR52, ciR298, and ciR133 can form circular RNAs in rice plants. RT-qPCR was also performed with the convergent

primer pair to examine the circRNAs responding to *Xoo* treatment (Fig. 3f). The result showed that the expression of the three circRNAs (ciR52, ciR298, and ciR133) could be induced by *Xoo* infection.

#### ciR133 is a circular RNA in rice plants

To further verify whether ciR133 is a circular RNA in rice, the back splicing junction site was first validated by Sanger sequencing (Fig. 4a). ciR133 is a 400 nt exonic circRNA, formed by the back-splicing of the 4th to 6th exon of its parental gene *OsARAB* (Os03g0320100/LOC\_Os03g20420), which encodes a putative  $\alpha$ -L-arabinofuranosidase (Fig. 4a).

Then, the circularity of ciR133 was further confirmed by RT-PCR using the divergent primer or the convergent primer (Fig. 4b). RNase R is known to degrade linear RNAs but not circRNAs, total RNAs were digested with RNase R for reverse transcription (RT) to further confirm circular ciR133. Therefore, only the circular ciR133 can be amplified using the RNase R-digested RNAs as template and the divergent primers for RT-PCR (Fig. 4b). However, even using the convergent primers for RT-PCR,

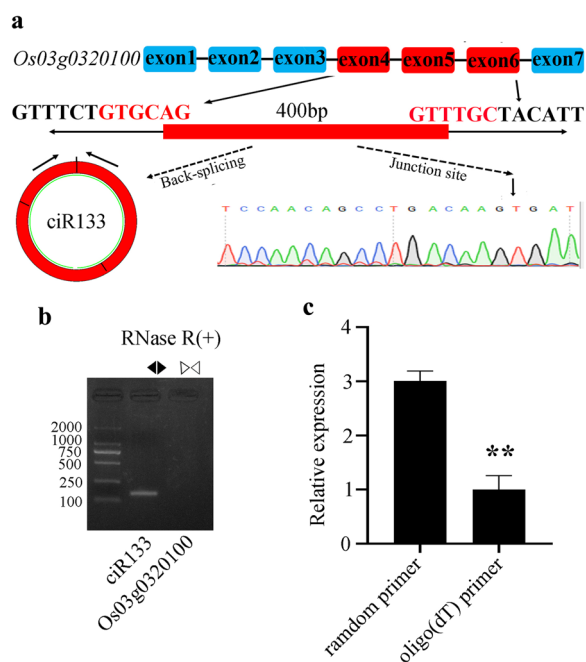


**Fig. 4** ciR133 is a non-coding circular RNA derived from *OsARAB*.

**a** Schematic diagram of ciR133 RNAs formed by back-splicing from the 4th, 5th and 6th exons of its parental gene *OsARAB*. **b** Validation of circular RNA formation of ciR133 by RT-PCR assays. Total RNAs of rice seedlings were treated with RNase R, and then used for the RT-PCR assays. **c** RT-qPCR analysis for ciR133 expression level in the *Xoo* infected rice leaves. RT for total RNAs were performed with random or oligo(dT) primers. *Os-eEF1-1a* was used as a reference gene. Means  $\pm$  SD represents the value with standard deviation ( $n = 3$  biological repeats,  $**P \leq 0.01$ )

the linear mRNA of *OsARAB* cannot be amplified using the RNase R-digested RNAs as a template (Fig. 4b).

Thirdly, because the circular RNAs lack poly (A) tail, the efficiency of RT using oligo (dT) as RT primer is lower than that using random primer. Therefore, RT-qPCR results showed that the expression level of the cDNA reverse-transcribed ciR133 by random primer was significantly higher than that using the cDNA reverse-transcribed ciR133 by oligo (dT) primers (Fig. 4c). This result indicates that ciR133 lacks a poly (A) tail which is usually present in protein coding genes. The above three results demonstrate that ciR133 can form a circular RNA in rice plants.

#### ciR133 represses the expression of its parental gene *OsARAB*

Does ciR133 regulate the expression of its parental gene *OsARAB*? We first analyzed the expression of ciR133 and *OsARAB* during *Xoo* infection (Fig. 5a). The results showed that the expression of ciR133 was induced, but the expression of *OsARAB* was repressed by *Xoo* (Fig. 5a), which indicates that ciR133 may repress expression of its parental gene *OsARAB* during *Xoo* infection. We then used a dual-luciferase system to analyze the interaction of ciR133 and *OsARAB* mRNA in tobacco plants (Fig. 5b). The fluorescence value of ciR133 and *OsARAB* co-transformed tobacco leaves was significantly lower than that of empty vector and *OsARAB* co-transformed tobacco leaves, indicating that ciR133 could negatively regulate expression of *OsARAB*. To further confirm this observation, we constructed the transgenic rice plants with over-expression (*ciR133-ox*) and down-expression (*Si-ciR133*) of circular ciR133, and with overexpression of its corresponding linear 133 (*Linear133-ox*) (Fig. 5b and Additional file 2: Figure S4). Overexpression of circular ciR133 in the *ciR133-ox* rice (Fig. 5c) resulted in repression of *OsARAB* expression (Fig. 5d). Conversely, repression of circular *ciR133* in the *Si-ciR133* rice (Fig. 5c) led to up-regulation of *OsARAB* expression (Fig. 5d). However, overexpression of linear ciR133 in *Linear133-ox* (Additional file 2: Figure S5b) did not alter expression of *ciR133* (Fig. 5c) or *OsARAB* (Fig. 5d). These results indicated that only circular ciR133 can repress the expression of its parental gene *OsARAB*.

#### Overexpression of *ciR133* or knocking out of *OsARAB* enhanced rice resistance against *Xoo* infection

The expression of ciR133 was highly induced by *Xoo* among the 3 DE circRNAs (Figs. 3f and 5a), prompting us to investigate the role of ciR133 that is derived from *OsARAB* in rice-*Xoo* interaction. To this end, the transgenic rice lines with overexpression (*OsARAB-ox*) and mutation (*Cri-ARAB*) of *OsARAB* were generated

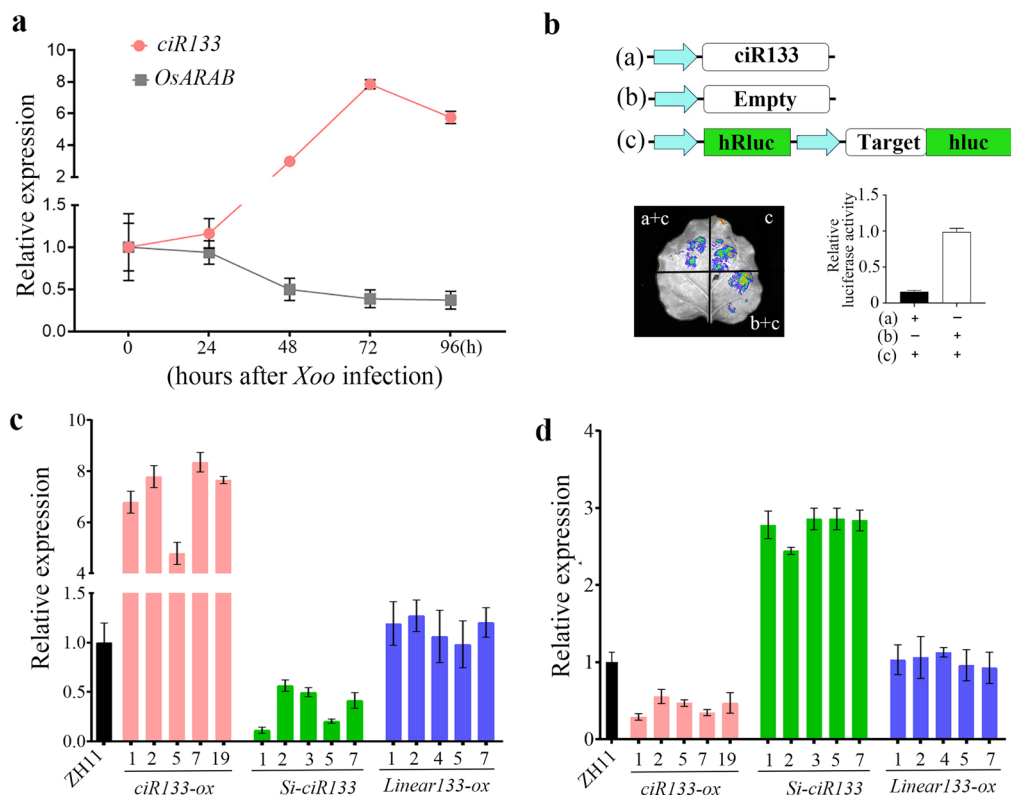


**Fig. 5** *ciR133* represses expression of *OsARAB* and responds to *Xoo* infection. **a** Expression change of *ciR133* and its parental gene *OsARAB* in four weeks old ZH11 plants after *Xoo* (AXO1947)-infection. **b** Dual-luciferase assay of interaction between *ciR133* and *OsARAB* in tobacco leaves. Schematic diagram of interaction construction was displayed in upper panel. Interaction of *ciR133* and *OsARAB* mRNA was displayed in left panel, and the luciferase activity was shown in right panel. *N. benthamiana* were grown at 30°C. The plants were infected for two days at 25°C. **c** Expression level of circular *ciR133* in the transgenic rice lines with overexpression of circular *ciR133* (*ciR133-ox*), down-expression of circular *ciR133* (*Si-ciR133*), and overexpression of linear *ciR133* (*Linear133-ox*). To confirm whether the circular *ciR133* RNAs were altered in these transgenic rice seedlings (*ciR133-ox* and *Si-ciR133*), their total RNAs were digested with RNase R for RT, and the divergent primers were used for qPCR assays. *Os-eEF1-1a* was used as a reference gene. **d** Expression change of *OsARAB* in *ciR133-ox*, *Si-ciR133*, and *Linear133-ox* seedlings. *Os-eEF1-1a* was used as a reference gene. Means ±SD represents the value with standard deviation (n=3 biological repeats)

(Additional file 2: Figure S5a, c). These transgenic rice lines were then selected for *Xoo* infection assays (Fig. 6). The results showed that the bacterial lesion lengths of *ciR133-ox* and *Cri-ARAB* transgenic rice plants were shorter than that of ZH11 (Fig. 6a, b). However, *Linear133-ox*, *Si-ciR133*, and *OsARAB-ox* transgenic rice plants did not show any differences in lesion length compared to ZH11. This result indicated that overexpression of *ciR133* or mutation of *OsARAB* could enhance rice resistance to *Xoo* infection. Nevertheless, these transgenic rice plants did not show any differences in major agronomic traits with ZH11 (Additional file 2: Figure S6). To further elucidate how *ciR133* is involved in *Xoo* resistance, we examined the expression of some defense-related genes. Three genes, the *OsPR10a*, *OsPR10b*, and *NAC4* that were reported by Li et al. (2014), were up-regulated in *ciR133-ox* and *Cri-ARAB* plants (Fig. 6c–e).

## Discussion

### Transcriptomic assay of rice leaves in response to *Xoo* infection

Bacterial leaf blight can cause a significant reduction to rice yield. Both mRNAs and ncRNAs function in regulating plant growth, development, and response to biotic and abiotic stresses. In this study, the rice variety ZH11 was monitored for responsive changes in transcriptome, including mRNAs and ncRNAs after infection of the *Xoo* strain AXO1947, which resulted in the identification of 31,698 protein-coding genes, 1341 circRNAs, 1060 lncRNAs, and 691 miRNAs in the rice plants (Additional file 1: Tables S2–S6). Of these, 4076 DE genes, 89 DE lncRNAs, 82 DE sRNAs, and 14 DE circRNAs were identified in *Xoo*-infected rice leaves (Additional file 1: Tables S2, S7–S10). The accuracy of the RNA-seq data was verified by the previously reported DE mRNAs (*OsS-WEET14* and *OsPR10a*) (Additional file 1: Table S12) and

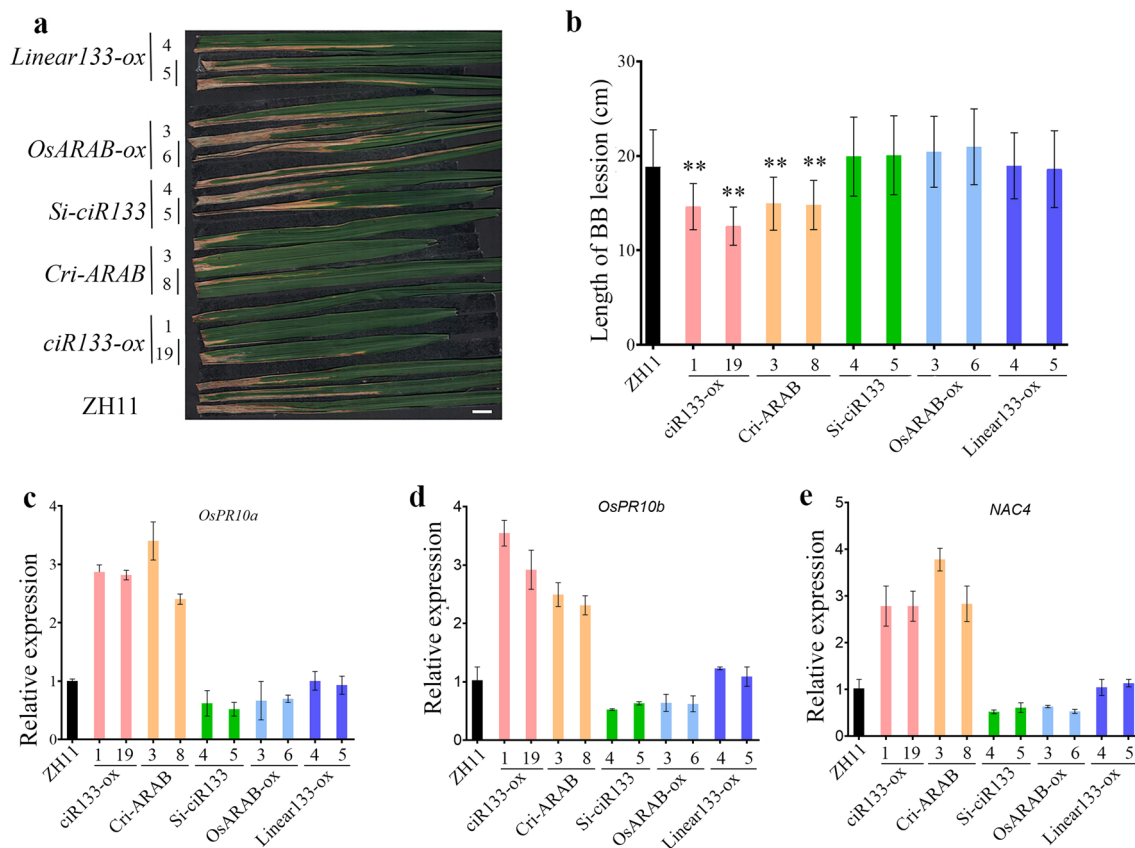


**Fig. 6** *ciR133* and *OsARAB* mediate disease resistance against *Xoo* infection in rice. **a, b** Phenotype (**a**) and lesion lengths (**b**) of the *ciR133* and *OsARAB* transgenic rice leaves after *Xoo*-infection. The 1.5 month-old rice leaves were inoculated with *Xoo* strain AXO1947 for 14 days. Scale bar = 1 cm in **a**. Means  $\pm$  SD in **b** represents value with standard deviation ( $n=3$  biological repeats),  $**P < 0.01$  in Student's *t*-test ( $n > 15$ ). **c–e** Relative expression of the pathogenesis related genes (*OsPR10a*, *OsPR10b*, and *NAC4*) in the transgenic rice plants. *OseEF1-a* was used as a reference gene. Means  $\pm$  SD represent the value with standard deviation ( $n=3$  biological repeats)

DE miRNAs (*osa-miR169a* and *osa-miR172*) (Additional file 1: Table S13) (Yu et al. 2018; Oliva et al. 2019), and confirmed by the results of some DE gene expression (Additional file 2: Figure S1). Combined analysis with all the DE mRNAs, circRNAs, lncRNAs, and miRNAs indicate that there was no co-targeted DE mRNAs of DE lncRNAs, miRNAs, and circRNAs, but there are 7 DE lncRNAs with the co-targeted DE mRNA and DE miRNAs, such as *Os06g0712200* which has been identified in a *Xoo* infection analysis (<http://systbio.cau.edu.cn>).

#### Transcriptional analysis of circRNAs in response to *Xoo* infection

circRNAs have been found to be involved in various stages of plant development, stress responses, and immune responses (Chen et al. 2019b). According to PLANTCIRCBASE v.7.0 (Xu et al. 2022), rice has been bioinformatically predicted to yield >40 k circRNAs, and RNA-seq was used to assembly the full-length sequences of 6519 circRNAs in rice seedlings (Chu

et al. 2022). Additionally, the *find\_circ* toolkit was used to predict 12,037 circRNAs in rice roots (Ye et al. 2015). Two years later, the same group used TopHat-Fusion software to predict 1046, 1328, and 1225 full-length sequences of circRNAs from three different public datasets (Ye et al. 2017). CIRI2 was used to observe 5723 and 3480 circRNAs in rice varieties IR25 and LTH, respectively (Fan et al. 2020). In IR25 young leaves, Fan et al. (2020) identified 2932 circRNAs and found that 636 circRNAs were specifically detected upon *M. oryzae* infection. Here, our results predicted 1341 circRNAs in rice seedlings (Additional file 1: Tables S2, S6), and 14 circRNAs showed differential expression after *Xoo* infection (Additional file 1: Tables S2, S10). Three DE circRNAs (*ciR52*, *ciR298*, and *ciR133*) were confirmed to form circular RNAs and respond to *Xoo* infection (Fig. 3d, e). These results imply that some circular RNAs play important roles in rice response to *Xoo* infection.

### Circular ciR133 may affect cell wall to attenuate *Xoo* infection

ciR133 is an exonic circRNA derived from its parental gene *OsARAB* (Fig. 4a), which is predicted to encode an  $\alpha$ -L-arabinofuranosidase, an enzyme that is involved in the degradation of lignocelluloses (Mondher and Narayan 2006). Previous studies have reported a certain extent of correlation between circRNAs and their parental genes (Pan et al. 2018). Although numerous circRNAs have been identified in plants by genome-wide analysis, few have been functionally characterized. *Xoo* infection induced expression of ciR133 and repressed expression of its parental gene *OsARAB* (Fig. 5a). Overexpression of ciR133 enhanced rice resistance against *Xoo* infection, and knocking out of *OsARAB* also increased rice resistance to *Xoo* infection (Fig. 6). This result suggests that ciR133 mediates disease resistance to *Xoo* infection through repression of *OsARAB* in rice, thereby maintaining cell wall integrity during *Xoo* infection (Sumiyoshi et al. 2013; Bacete et al. 2018; Drula et al. 2022). Therefore, we proposed that *Xoo*-induced ciR133 expression may repress expression of *OsARAB*. As a result, ciR133-overexpression and the knocking out of *OsARAB* could reinforce cell wall integrity in response to *Xoo* infection. The arabinofuranosidase is also considered as a virulence factor of *Sclerotinia sclerotiorum* to cause canola necrosis in leaves and stems, and disruption of the encoding gene of its arabinofuranosidase reduced *S. sclerotiorum* virulence on canola tissue (Yajima et al. 2009). Likewise, *Xoo*-induced ciR133 may also repress the *Xoo*-arabinofuranosidase expression and reduced its virulence on rice. In addition, three pathogenesis-related genes (*OsPR10a*, *OsPR10b*, and *NAC4*) (Li et al. 2014) were induced in ciR133-ox and Cri-*ARAB* plants (Fig. 6c–e), which may also contribute to the resistance to *Xoo*.

## Methods

### Plant materials and growth conditions

Rice cultivar Zhonghua 11 (*Oryza sativa* L. ssp. *Japonica*, ZH11) was used in this study. Seeds were germinated in the dark for 3 days, then the germinated seeds were planted in pots or grown under optimum conditions in the green house in South China Botanical Garden, Chinese Academy of Sciences, under natural light (12 h light/12 h darkness) and temperature (25–35°C). Four weeks old plants were used for *Xoo* inoculation.

### Bacterial blight strains and inoculation assays

Virulent *Xoo* strain AXO1947 that is obtained from Africa (Gu et al. 2004) were cultivated on PSA medium (10 g/L peptone, 10 g/L sucrose, 1 g/L glutamic acid, 16 g/L agar, pH 7.0) at 28°C under darkness for 2 days.

Bacteria were collected and re-suspended in sterile water at an  $OD_{600}=0.5$  for inoculation of rice leaves. The bacteria were injected into the leaves with a syringe. The inoculated rice leaves were harvested 48 h later and were immediately frozen in liquid nitrogen, then stored at  $-80^{\circ}\text{C}$  for further analysis. The leaves with the mock treatment were harvested and used as a control. Each treatment has three replicates. Bacterial blight inoculation was performed with the leaf-clipping method as previously described (Zeng et al. 2020). Bacterial lesion lengths were measured at two weeks post inoculation.

### Total RNA isolation, library preparation, and RNA sequencing

A total of 0.5 g leaves was taken from three plants and mixed together as one sample. The total RNAs were isolated and extracted using RNA TRIzol DP411 (Tiangen, Beijing, China), followed by the manufacturer's instructions. Quantity of total RNAs were conducted by NanoDrop 2000 (Thermo Fisher Scientific, New York, USA) and its integrity was detected by LabChip GX (Agilent2100, CA, USA) with  $RIN \geq 6.5$ . High quality of total RNAs from leaves were mixed and sent to Bio-Marker Technologies (Beijing, China) for library construction and sequencing.

### Library preparation for mRNA, lncRNA, and circRNA sequencing

For mRNA, lncRNA, and circRNA sequencing, about 1.5  $\mu\text{g}$  RNA per sample was used as input and the rRNA was removed using the Ribo-Zero rRNA Removal Kit (Epicentre, Madison, WI, USA). Sequencing libraries were generated using NEBNextR UltraTM Directional RNA Library Prep Kit for IlluminaR (NEB, USA). Fragmentation was carried out using divalent cations under elevated temperature in NEBNext First Strand Synthesis Reaction Buffer (5 $\times$ ). First strand cDNA was synthesized using random hexamer primer and reverse transcriptase. Second-strand cDNA synthesis was subsequently performed using DNA Polymerase I and RNase H. Remaining overhangs were converted into blunt ends via exonuclease/polymerase activities. After adenylation of 3' ends of DNA fragments, NEBNext adaptor with hairpin loop structure were ligated to prepare for hybridization. In order to select insert fragments of preferentially 150~200 bp in length, the library fragments were purified with AMPure XP Beads (Beckman Coulter, Beverly, USA). Then 3  $\mu\text{L}$  USER Enzyme (NEB, USA) was used with size-selected, adaptor-ligated cDNA at 37°C for 15 min before PCR. Then PCR was performed with Phusion High-Fidelity DNA polymerase, Universal PCR primers and Index (X) Primer. Finally, PCR products

were purified with AMPure XP system (Beckman Coulter, Suzhou, China) and library quality was assessed on the Agilent Bioanalyzer 2100 (Agilent, Berlin, German).

#### Library preparation for sRNA sequencing

A total of 2.5 ng RNA per sample was used as input material for the RNA sample preparation. Sequencing libraries were generated using SRNA Library Construction SOP by BMK-2020 version (BioMarker Technologies, Beijing, China). First, the 3'SR Adaptor was ligated with the RNA. Mixed 3'SR adaptor, RNA and nuclease-free water were incubated for 2 min at 70°C in a preheated thermal cycler. The mixture was then transferred on ice. Then, 3'Ligation Reaction Buffer (2×) and 3'Ligation Enzyme Mix were added to ligate the 3'SR adaptor. In order to prevent the formation of adaptor-dimer, the SR RT Primer was utilized to hybridize with the excess of 3'SR adaptor that remains unbound after the 3'ligation reaction. This hybridization process transforms the single-stranded DNA adaptor into a double-stranded DNA molecule. The double-stranded DNAs are not suitable substrates for ligation-mediated reactions. Then the ligation of the 5'SR Adaptor, followed by the synthesis of the first chain through reverse transcription. Finally, PCR amplification and size selection were performed. For fragment screening, PAGE gel electrophoresis was employed, and rubber cutting was used to recycle the pieces that contained small RNA libraries. Finally, PCR products were purified using AMPure XP system and library quality was assessed on the Agilent Bioanalyzer 2100 system.

#### Clustering and sequencing

Clustering of the index-coded samples was performed on a cBot Cluster Generation System using TruSeq PE Cluster Kitv3-cBot-HS (Illumina) according to the manufacturer's instructions. After cluster generation, the library preparations were sequenced on an Illumina platform and reads were generated.

#### Reads mapping and transcriptomic assembly

Quality control was performed using FastQC (de Sena Brandine and Smith 1874). RNA-seq paired-end reads were aligned to the rice IRGSP-1.0 genome (RAP-DB|HOME (affrc.go.jp) via TopHat (Trapnell et al. 2009) and assembled via Cufflinks (Trapnell et al. 2010). Prediction and identification of mRNAs, lncRNAs, and circRNAs were performed with visual pipeline described in Fig. 1b. The transcriptome was assembled using the StringTie (<https://ccb.jhu.edu/software/stringtie/index.shtml>), based on the reads that are mapped to the reference genome. The assembled transcripts were annotated using the gffcompare program (<http://ccb.jhu.edu/software/stringtie/gffcompare.shtml>).

The unknown transcripts were used to screen putative lncRNAs. Three computational approaches including CPC/Pfam/CPAT were combined to sort non-protein coding RNA candidates from putative protein-coding RNAs in the unknown transcripts (Bateman et al. 2004; Kong et al. 2007; Wang et al. 2013). Putative protein-coding RNAs were filtered using minimum length and exon number threshold. Genes with lengths more than 200 nt and contain more than two exons were selected as lncRNA candidates and were further screened using CPC/Pfam/CPAT that can distinguish the protein-coding genes from the non-coding genes. The different types of lncRNAs, including lincRNA, intronic lncRNA, anti-sense lncRNA, sense lncRNA, were selected using cuffcompare program. The unmapped reads were used to predict circRNAs.

We used CIRI2 (CircRNA Identifier) tools (Gao et al. 2015) and find\_circ (Memczak et al. 2013) to identify circRNA. It scans SAM files twice and collects sufficient information to identify and characterize circRNAs. Briefly, during the first scan of SAM alignment, CIRI detects junction reads with PCC signals that reflect a circRNA candidate. Preliminary filtering is implemented using paired-end mapping (PEM) and GT-AG splicing signals for junctions. After clustering junction reads and recording each circRNA candidate, CIRI scans the SAM alignment again to detect additional junction reads and meanwhile performs further filtering to eliminate false positive candidates resulting from incorrectly mapped reads of homologous genes or repetitive sequences. Finally, the identified circRNAs are output with annotation information. We used TargetFinder tools (<https://github.com/carringtonlab/TargetFinder>) to predict target miRNA.

Small RNA-Seq data were analyzed using Bowtie (<https://bowtie-bio.sourceforge.net/bowtie2/manual.shtml#command-line>). The generated reads were subjected to sequence alignment against the Silva (<https://bio.tools/silva#/>), GtRNADB (<http://gtrnadb.ucsc.edu/>), Rfam (<https://rfam.org/>), and Rfam databases (<https://www.girinst.org/replib/>), followed by filtering of ribosomal RNA (rRNA), transfer RNA (tRNA), small nuclear RNA (snRNA), small nucleolar RNA (snoRNA), other non-coding RNA (ncRNA), and repeats. The remaining reads were used to detect known miRNAs and novel miRNAs predicted by comparing with known miRNAs from miRBase (<https://www.mirbase.org/>). Randfold tools soft (<https://hpc.ilri.cgiar.org/randfold-software>) was used for novel miRNA secondary structure prediction.

#### DE mRNAs and ncRNAs analysis

DESeq R package (1.10.1) (Robinson et al. 2010) was utilized to establish the expression levels of all transcripts.

The  $P$ -value  $< 0.05$  and  $\log_2$  (fold change, FC)  $\geq 1.0$  were set as the cut-off criteria for identifying the DE-mRNAs, DE-miRNAs, DE-lncRNAs, and DE-circRNAs.

#### RT-qPCR

Total RNAs from leaves before and after inoculation with *Xoo* was extracted using a TRIzol kit (Invitrogen, USA), and were reverse transcribed into cDNA using an M-MLV RT Kit (Accurate Biotechnology, AG11711, China). For RT of mRNAs and lncRNAs, the oligo(dT) primers were used. For RT of miRNAs, the specific stem-loop primers were used. For RT of circRNAs, total RNAs were treated at 37°C with 3 U/ $\mu$ g of RNase R (Epicentre Biotechnologies, Madison, WI, USA) for 30 min, and the random 6-mer primers were used.

For qPCR, the divergent primers for detecting circRNAs and the convergent primers for detecting linear RNAs were designed using Primer 3 (version 0.4.0) (<http://bioinfo.ut.ee/primer3-0.4.0/>). The above cDNAs were used as templates for qPCR with SYBR qPCR Real Master Mix (ChamQ Universal, China) on LightCycler 480 (Roche, USA). *OseEF1-a* was used as the reference gene for mRNAs, lncRNAs, and circRNAs, and *U6* was used as the reference gene for miRNAs.

#### Validation of the circular RNAs by RT-PCR assays

To verify circular RNAs, the total RNAs were treated with or without RNase R for RT assay, and the divergent primers and convergent primers were designed for PCR assays. The divergent primers of PCR could only amplify bands using the circular cDNAs as the template, but not using genomic DNAs (gDNAs) as template; while the convergent primers could amplify bands using both linear cDNAs and gDNAs as templates (primer pairs as in Fig. 3d). The PCR reaction was performed using 2 $\times$ Taq Plus Mix (Vazyme, China) according to the manufacturer's protocol. Sanger sequencing of these PCR bands was performed after purifying PCR products using DNA Gel Extraction Kit (Tsingke Biotechnology, China) according to the manufacturer's protocol.

#### Construction of transgenic rice with overexpression of circular and linear *ciR133*

Due to the circular nature of circRNAs, the construction methods of overexpression and interference vectors are slightly different from those of the coding genes. For overexpression of circular *ciR133* and *liner133*, the vector construction was performed as following process. The full length of *ciR133* and the target fragments from the start site of the upstream intron to the end site of the downstream intron of *ciR133* were cloned using the specific primers. The genomic region of *ciR133* was amplified from ZH11 gDNA, and the cognate linear

fragment of *ciR133* was amplified from ZH11 cDNA. The specific primer pairs for cloning *ciR133* and linear fragment are both with restriction endonuclease of *Bgl* II and *BstE* II, respectively. The fragments were then cloned into pCAMBIA1301 vectors under the control of *Cauliflower mosaic virus 35S* promoter to generate the recombinant plasmids of pCAMBIA1301-*ciR133* and pCAMBIA1301-*35S:linear133*, respectively (Additional file 2: Figure S4). The full length of *ciR133* and its cognate linear fragment were validated by Sanger sequencing.

For RNAi of circular *ciR133*, the vector construction was performed as following process. The circRNA back-to-back splice site is the only difference from the parental gene transcript. RNAi technology can not only effectively inhibit the expression of circRNA, but also ensure that the parental gene transcription is not affected. Taking 20 nt before and after the back-to-back splicing site after *ciR133* looping as the target sequence, the primers were designed and cloned into the intermediate vector pNW55 using the artificial microRNA technology (<http://wmd3.weigelworld.org/cgi-bin/webapp.cgi>), and then sub-cloned into vector pCAMBIA1301 at *Bgl*II and *Afl*III digestion sites.

*Agrobacterium tumefaciens* strain EHA105 containing plasmids were transformed into ZH11. Rice transformation of ZH11 was performed as previously described (Hiei et al. 1994). Positive transgenic lines were confirmed by a hygromycin sensitivity test as well as by amplifying the *Hpt*. Expression levels of circRNA133 in the transgenic rice lines that overexpress *ciR133* (*ciR133-ox*) or linear *ciR133* (*35S:linear 133-ox*) were further confirmed by RT-qPCR assays.

#### Mutation and overexpression of *OsARAB* in rice

Mutation of *OsARAB* (LOC\_Os03g20420) were implemented using the CRISPR/Cas9 genome editing system (Ma et al. 2015). The anchor sequence was targeted to the 7th exon of *OsARAB*. gDNA templates of the transformed rice plants were extracted, and the editing site was amplified by PCR using a pair of flanking primers. The PCR products were sequenced and analyzed using DSDecode (Ma et al. 2015) to confirm *OsARAB* deletion. To further confirm the edited sequence, RT-PCR products from the mutated *OsARAB* seedlings were sequenced again. To construct *OsARAB* -overexpressing plants (*OsARAB-ox*), a 822 bp *OsARAB* cDNA fragment containing the open reading frame (ORF) was inserted downstream of the 35S promoter in pCambia1301 at *Afl*III and *Bgl*II digestion sites to produce the plasmid p35S-*OsARAB*, and then the vectors were transferred into *A. tumefaciens* strain EHA105 to transform ZH11.

All the primers used in this study are listed in Additional file 1: Table S14. IBM SPSS 20.0 software was used to determine the statistical significance of the data.

#### Abbreviations

circRNA	Circular RNA
CRISPR/Cas9	Clustered regularly interspaced short palindromic repeat/CRISPR-associated nuclease 9
lncRNA	Long non-coding RNA
miRNA	MicroRNA
ncRNA	Non-coding RNA
OsARAB	<i>Oryza sativa</i> Arabinofuranosidase
RT-qPCR	Real time quantitative-PCR
Xoo	<i>Xanthomonas oryzae</i> pv. <i>Oryzae</i>

#### Supplementary Information

The online version contains supplementary material available at <https://doi.org/10.1186/s42483-023-00188-8>.

**Additional file 1: Table S1.** Summary statistic for sequence quality control and mapped data of samples. **Table S2.** Summary of whole RNA seq data. **Tables S3–S6.** List of all mRNAs (S3), lncRNAs (S4), miRNAs (S5), and circRNAs (S6) from the ZH11 seedling before and after 48 hours Xoo infection. **Tables S7–S10.** List of all DE mRNAs (S7), lncRNAs (S8), miRNAs (S9), and circRNAs (S10) after 48 hours Xoo infection. **Table S11.** Combined analysis of DE lncRNAs with DE miRNAs and DE mRNAs. **Table S12.** DE genes confirmed by RT-qPCR assays. **Table S13.** DE miRNAs confirmed by RT-qPCR assays. **Table S14.** List of all primers.

**Additional file 2: Figure S1.** RT-qPCR verification of the differentially expressed genes identified by RNA-seq. **Figure S2.** Venn diagram of DE lncRNAs, miRNAs, and Cis-mRNAs (a), Trans-mRNAs (b), and KEGG pathway enrichment analysis of DE lncRNAs annotated by its targeted mRNAs (c). **Figure S3.** KEGG pathway enrichment analysis of miRNAs annotated by its targeted mRNAs. **Figure S4.** Construction of the circular ciR133 overexpression and knockdown vector. **Figure S5.** Molecular analysis of OsARAB over-expression and RNAi transgenic rice and linear133 overexpression rice plants. **Figure S6.** Statistical analysis of the main agronomic traits for transgenic rice lines of ciR133 and OsARAB.

#### Acknowledgements

We thank Mr. YS Wang and Ms. XX Zhang for helping us to manage the rice plants.

#### Authors' contributions

KX, XZ, and MZ conceived the project and wrote the manuscript. XP and KX performed most of the experiments, and XZ performed part of the work. All authors read and approved the final manuscript.

#### Funding

This work was supported by the Strategic Priority Research Program of Chinese Academy of Science (XDA24030201), the National Natural Science Foundation of China (32171933, 31971816), and the Guangzhou Science and Technology Project (202102021003, 2023B03J0742).

#### Availability of data and materials

All the data were available at the DDBJ database (BioProject Accession: PRJDB14902).

#### Declarations

##### Ethics approval and consent to participate

Not applicable.

##### Consent for publication

Not applicable.

#### Competing interests

The authors declare that they have no competing interests.

Received: 3 March 2023 Accepted: 4 July 2023

Published online: 21 July 2023

#### References

- Adhikari TB, Cruz C, Zhang Q, Nelson RJ, Skinner DZ, Mew TW, et al. Genetic diversity of *Xanthomonas oryzae* pv. *oryzae* in Asia. *Appl Environ Microbiol.* 1995;61:966–71. <https://doi.org/10.1128/aem.61.3.966-971.1995>.
- Ahmed T, Shahid M, Noman M, Niazi MBK, Mahmood F, Manzoor I, et al. Silver nanoparticles synthesized by using *Bacillus cereus* SZT1 ameliorated the damage of bacterial leaf blight pathogen in rice. *Pathogens.* 2020;9:160–77. <https://doi.org/10.3390/pathogens9030160>.
- Bacete L, Melida H, Miedes E, Molina A. Plant cell wall-mediated immunity: cell wall changes trigger disease resistance responses. *Plant J.* 2018;93:614–36. <https://doi.org/10.1111/tpj.13807>.
- Bateman A, Coin L, Durbin R, Finn RD, Hollich V, Griffiths-Jones S, et al. The Pfam protein families database. *Nucleic Acids Res.* 2004;32:D138–41. <https://doi.org/10.1093/nar/gkh121>.
- de Sana Brandine G, Smith AD, Falco: high-speed FastQC emulation for quality control of sequencing data. *F1000Res.* 2019;8:1874. <https://doi.org/10.12688/f1000research.21142.2>.
- Brown DM, Zeef LAH, Ellis J, Goodacre R, Turner SR. Identification of novel genes in *Arabidopsis* involved in secondary cell wall formation using expression profiling and reverse genetics. *Plant Cell.* 2005;17:2281–95. <https://doi.org/10.1105/tpc.105.031542>.
- Buddhachat K, Sripairoj N, Ritbamrung O, Inthima P, Ratanasut K, Boonsrangsom T, et al. RPA-assisted Cas12a system for detecting pathogenic *Xanthomonas oryzae*, a causative agent for bacterial leaf blight disease in rice. *Rice Sci.* 2022;2022(29):340–52. <https://doi.org/10.1016/j.rsci.2021.11.005>.
- Cao YR, Zhang Y, Chen YY, Yu N, Liaqat S, Wu WX, et al. *OsPG1* encodes a polygalacturonase that determines cell wall architecture and affects resistance to bacterial blight pathogen in rice. *Rice.* 2021;14:36. <https://doi.org/10.1186/s12284-021-00478-9>.
- Chen L, Kong R, Wu C, Wang S, Liu Z, Liu S, et al. Circ-MALAT1 functions as both an mRNA translation brake and a microRNA sponge to promote self-renewal of hepatocellular cancer stem cells. *Adv Sci (weinh).* 2019a;7:1900949. <https://doi.org/10.1002/adv.201900949>.
- Chen X, Yang T, Wang W, Xi W, Zhang T, Li Q, et al. Circular RNAs in immune responses and immune diseases. *Theranostics.* 2019b;9:588–607. <https://doi.org/10.7150/thno.29678>.
- Chu Q, Ding Y, Xu X, Ye CY, Zhu QH, Guo L, et al. Recent origination of circular RNAs in plants. *New Phytol.* 2022;233:515–25. <https://doi.org/10.1111/nph.17798>.
- Conn VM, Hugouvieux V, Nayak A, Conos SA, Capovilla G, Cildir G, et al. A circRNA from SEPALLATA3 regulates splicing of its cognate mRNA through R-loop formation. *Nat Plants.* 2017;3:1–5. <https://doi.org/10.1038/nplants.2017.53>.
- Drula E, Garron ML, Dogan S, Lombard V, Henrissat B, Terrapon N. The carbohydrate-active enzyme database: functions and literature. *Nucleic Acids Res.* 2022;50:D571–7. <https://doi.org/10.1093/nar/gkab1045>.
- Fan J, Quan W, Li GB, Hu XH, Wang Q, Wang H, et al. circRNAs are involved in the rice-*Magnaporthe oryzae* interaction. *Plant Physiol.* 2020;182:272–86. <https://doi.org/10.1104/pp.19.00716>.
- Feng J, Chen K, Dong X, Xu X, Jin Y, Zhang X, et al. Genome-wide identification of cancer-specific alternative splicing in circRNA. *Mol Cancer.* 2019;18:35–41. <https://doi.org/10.1186/s12943-019-0996-0>.
- Gao Y, Wang JF, Zhao FQ. CIRI: an efficient and unbiased algorithm for de novo circular RNA identification. *Genome Biol.* 2015;16:4. <https://doi.org/10.1186/s13059-014-0571-3>.
- Gu K, Tian D, Yang F, Wu L, Sreekala C, Wang D, et al. High-resolution genetic mapping of *Xa27(t)*, a new bacterial blight resistance gene in rice *Oryza sativa* L. *Theor Appl Genet.* 2004;108:800–7. <https://doi.org/10.1007/s00122-003-1491-x>.
- Hansen TB, Wiklund ED, Bramsen JB, Villadsen SB, Statham AL, Clark SJ, et al. miRNA-dependent gene silencing involving Ago2-mediated cleavage

- of a circular antisense RNA. *EMBO J*. 2011;30:4414–22. <https://doi.org/10.1038/emboj.2011.359>.
- Hashimoto K, Yoshida M, Hasumi K. Isolation and characterization of CcAbf62A, a GH62 alpha-L-arabinofuranosidase, from the basidiomycete *Coprinopsis cinerea*. *Biosci Biotechnol Biochem*. 2011;75:342–5. <https://doi.org/10.1271/bbb.100434>.
- Hiei Y, Ohta S, Komari T, Kumashiro KT. Efficient transformation of rice (*Oryza sativa* L.) mediated by *Agrobacterium* and sequence analysis of the boundaries of the T-DNA. *Plant J*. 1994;6:271–82. <https://doi.org/10.1046/j.1365-3113x.1994.6020271.x>.
- Kong L, Zhang Y, Ye ZQ, Liu XQ, Zhao SQ, Wei L, et al. CPC: assess the protein-coding potential of transcripts using sequence features and support vector machine. *Nucleic Acids Res*. 2007;35:W345–9. <https://doi.org/10.1093/nar/gkm391>.
- Lai X, Bazin J, Webb S, Crespi M, Zubieta C, Conn SJ. CircRNAs in plants. *Adv Exp Med Biol*. 2018;1087:329–43. [https://doi.org/10.1007/978-981-13-1426-1\\_26](https://doi.org/10.1007/978-981-13-1426-1_26).
- Li Y, Lu YG, Shi Y, Wu L, Xu YJ, Huang F, et al. Multiple rice microRNAs are involved in immunity against the blast fungus *Magnaporthe oryzae*. *Plant Physiol*. 2014;164:1077–92. <https://doi.org/10.1104/pp.113.230052>.
- Li X, Yang L, Chen LL. The biogenesis, functions, and challenges of circular RNAs. *Mol Cell*. 2018;71:428–42. <https://doi.org/10.1016/j.molcel.2018.06.034>.
- Liu M, Shi Z, Zhang X, Wang M, Zhang L, Zheng K, et al. Inducible overexpression of *Ideal Plant Architecture 1* improves both yield and disease resistance in rice. *Nat Plants*. 2019;5:389–400. <https://doi.org/10.1038/s41477-019-0383-2>.
- Lu J, Wang C, Zhang FZ, Zeng D, Zhou Y. Comparative microRNA profiling reveals microRNAs involved in rice resistant response to bacterial blight. *Crop J*. 2021;9:834–42. <https://doi.org/10.1016/j.cj.2020.08.009>.
- Ma X, Zhang Q, Zhu Q, Liu W, Chen Y, Qiu R, et al. A Robust robust CRISPR/Cas9 system for convenient, high-efficiency multiplex genome editing in monocot and dicot plants. *Mol Plant*. 2015;8:1274–84. <https://doi.org/10.1016/j.molp.2015.04.007>.
- Maruyama R, Mayuzumi Y, Morisawa J, Kawai S. Transgenic rice plants expressing the alpha-L-arabinofuranosidase of *Coprinopsis cinerea* exhibit strong dwarfism and markedly enhanced tillering. *Plant Biotechnol (tokyo)*. 2021;38:379–86. <https://doi.org/10.5511/plantbiotechnology.21.0616a>.
- Memczak S, Jens M, Elefsinioti A, Torti F, Krueger J, et al. Circular RNAs are a large class of animal RNAs with regulatory potency. *Nature*. 2013;495:333–8. <https://doi.org/10.1038/nature11928>.
- Mondher N, Narayan B. Alpha-L-Arabinofuranosidases: the potential applications in biotechnology. *J Ind Microbiol Biotechnol*. 2006;33:247–60. <https://doi.org/10.1007/s10295-005-0072-1>.
- Oliva R, Ji C, Atienza-Grande G, Huguet-Tapia JC, Perez-Quintero A, Li T, et al. Broad-spectrum resistance to bacterial blight in rice using genome editing. *Nat Biotechnol*. 2019;37:1344–50. <https://doi.org/10.1038/s41587-019-0267-z>.
- Pan T, Sun XQ, Liu YY, Li H, Deng GB, Lin HH, et al. Heat stress alters genome-wide profiles of circular RNAs in *Arabidopsis*. *Plant Mol Biol*. 2018;96:217–29. <https://doi.org/10.1007/s11103-017-0684-7>.
- Pruitt RN, Schwessinger B, Joe A, Thomas N, Liu FR, Albert M, et al. The rice immune receptor *XA21* recognizes a tyrosine-sulfated protein from a Gram-negative bacterium. *Sci Adv*. 2015;1:e1500245. <https://doi.org/10.1126/sciadv.1500245>.
- Robinson MD, McCarthy DJ, Smyth GK. edgeR: a bioconductor package for differential expression analysis of digital gene expression data. *Bioinformatics*. 2010;26:139–40. <https://doi.org/10.1093/bioinformatics/btp616>.
- Song L, Fang Y, Chen L, Wang J, Chen X. Role of non-coding RNAs in plant immunity. *Plant Commun*. 2021;2:100180. <https://doi.org/10.1016/j.xplc.2021.100180>.
- Sumiyoshi M, Nakamura A, Nakamura H, Hakata M, Ichikawa H, Hirochika H, et al. Increase in cellulose accumulation and improvement of saccharification by overexpression of arabinofuranosidase in rice. *PLoS ONE*. 2013;8:e78269. <https://doi.org/10.1371/journal.pone.0078269>.
- Sun X, Cao Y, Yang Z, Xu C, Li X, Wang S, et al. *Xa26*, a gene conferring resistance to *Xanthomonas oryzae* pv. *oryzae* in rice, encodes an LRR receptor kinase-like protein. *Plant J*. 2004;37:517–27. <https://doi.org/10.1046/j.1365-3113x.2003.01976.x>.
- Takahashi T, Diener T. Potato spindle tuber viroid: XIV. Replication in nuclei isolated from infected leaves. *Virology*. 1975;64:106–14. [https://doi.org/10.1016/0042-6822\(75\)90083-5](https://doi.org/10.1016/0042-6822(75)90083-5).
- Trapnell C, Pachter L, Salzberg SL. TopHat: discovering splice junctions with RNA-Seq. *Bioinformatics*. 2009;25:1105–11. <https://doi.org/10.1093/bioinformatics/btp120>.
- Trapnell C, Williams BA, Pertea G, Mortazavi A, Kwan G, Van Baren MJ, et al. Transcript assembly and quantification by RNA-Seq reveals unannotated transcripts and isoform switching during cell differentiation. *Nat Biotechnol*. 2010;28:511–5. <https://doi.org/10.1038/nbt.1621>.
- Wang L, Park HJ, Dasari S, Wang S, Kocher JP, Li W. CPAT: Coding-potential assessment tool using an alignment-free logistic regression model. *Nucleic Acids Res*. 2013;41:e74. <https://doi.org/10.1093/nar/gkt006>.
- Wang CL, Zhang XP, Fan YL, Gao Y, Zhu QL, Zheng CK, et al. *XA23* is an executor R protein and confers broad-spectrum disease resistance in rice. *Mol Plant*. 2015;8:290–302. <https://doi.org/10.1016/j.molp.2014.10.010>.
- Wang J, Tian D, Gu K, Yang X, Wang L, Zeng X, et al. Induction of *Xa10*-like genes in rice cultivar nipponbare confers disease resistance to rice bacterial blight. *Mol Plant Microbe Interact*. 2017;30:466–77. <https://doi.org/10.1094/MPMI-11-16-0229-R>.
- Xie WY, Ke YG, Cao JB, Wang SP, Yuan M. Knock out of transcription factor *WRKY53* thickens sclerenchyma cell walls, confers bacterial blight resistance. *Plant Physiol*. 2021;187:1746–61. <https://doi.org/10.1093/plphys/kiab400>.
- Xu X, Du T, Mao W, Li X, Ye CY, Zhu QH, et al. PlantcircBase 7.0: full-length transcripts and conservation of plant circRNAs. *Plant Commun*. 2022;3:100343. <https://doi.org/10.1016/j.xplc.2022.100343>.
- Yajima W, Liang Y, Kav NN. Gene disruption of an arabinofuranosidase/beta-xylosidase precursor decreases *Sclerotinia sclerotiorum* virulence on canola tissue. *Mol Plant Microbe Interact*. 2009;22:783–9. <https://doi.org/10.1094/MPMI-22-7-0783>.
- Ye CY, Chen L, Liu C, Zhu QH, Fan LJ. Widespread noncoding circular RNAs in plants. *New Phytol*. 2015;208:88–95. <https://doi.org/10.1111/nph.13585>.
- Ye CY, Zhang X, Chu Q, Liu C, Yu Y, Jiang W, et al. Full-length sequence assembly reveals circular RNAs with diverse non-GT/AG splicing signals in rice. *RNA Biol*. 2017;14:1055–63. <https://doi.org/10.1080/15476286.2016.1245268>.
- Yoshimura S, Yamanouchi U, Katayose Y, Toki S, Wang ZX, Kono I, et al. Expression of *Xa1*, a bacterial blight-resistance gene in rice, is induced by bacterial inoculation. *Proc Natl Acad Sci U S A*. 1998;95:1663–8. <https://doi.org/10.1073/pnas.95.4.1663>.
- Yu C, Chen Y, Cao Y, Chen H, Wang J, Bi YM, et al. Overexpression of miR169o, an overlapping microrna in response to both nitrogen limitation and bacterial infection, promotes nitrogen use efficiency and susceptibility to bacterial blight in rice. *Plant Cell Physiol*. 2018;59:1234–7. <https://doi.org/10.1093/pcp/pcy060>.
- Yu Y, Zhou YF, Feng YZ, He H, Lian JP, Yang YW, et al. Transcriptional landscape of pathogen-responsive lncRNAs in rice unveils the role of *ALEX1* in jasmonate pathway and disease resistance. *Plant Biotech J*. 2020;18:679–90. <https://doi.org/10.1111/pbi.13234>.
- Zeng X, Luo Y, Vu NQ, Shen S, Xia K, Zhang M. CRISPR/Cas9-mediated mutation of *OsSWEET14* in rice cv. Zhonghua11 confers resistance to *Xanthomonas oryzae* pv. *oryzae* without yield penalty. *BMC Plant Biol*. 2020;20:313. <https://doi.org/10.1186/s12870-020-02524-y>.
- Zhang JM, Wang T, Wang C, Zhang W, Yang L. Identification and expression analysis of *OsmiR1861k* in rice leaves in response to *Xanthomonas oryzae* pv. *oryzae*. *J Gen Plant Pathol*. 2015;81:108–17. <https://doi.org/10.1007/s10327-015-0579-x>.
- Zhao Q, Dixon RA. Altering the cell wall and its impact on plant disease: from forage to bioenergy. *Annu Rev Phytopathol*. 2014;52:69–91. <https://doi.org/10.1146/annurev-phyto-082712-102237>.